www.lpr-journal.org

LASER & PHOTONICS REVIEWS

WILEY-VCH

REPRINT

LASER
& PHOTONICS
REVIEWS

Laser Photonics Rev. **8,** No. 6, 889–895 (2014) / **DOI** 10.1002/lpor.201400055

Abstract Robust high-power narrow-linewidth lasers at 589 nm are required for sodium laser guide star adaptive optics in astronomy. A high-power 589 nm laser based on Raman fiber amplifier is reported here, which works in both continuous-wave and pulsed formats. In the continuous-wave case, the laser produces more than 50 W output. In the pulsed case, the same laser produces square-shaped pulses with tunable repetition rate (500 Hz to 10 kHz) and duration (1 ms to 30 μs). The peak power is as high as 84 W and remains constant during the tuning. The laser also emits an adjustable sideband at 1.71 GHz away from the main laser frequency for better sodium excitation. The versatility of the laser offers much flexibility in laser guide star application.

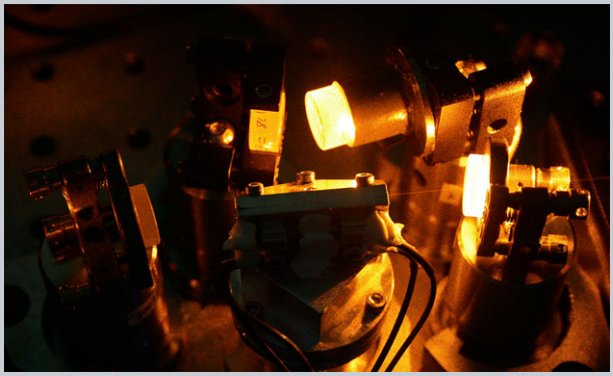

ORIGINAL
PAPER

Versatile Raman fiber laser for sodium laser guide star

Lei Zhang[1,2], Huawei Jiang[1,2], Shuzhen Cui[1], Jinmeng Hu[1,2], and Yan Feng[1,*]

1. Introduction

The effects of atmospheric turbulence can greatly degrade the astronomical imaging on large ground-based astronomical telescopes. Fortunately, it can be practically eliminated in real time by the laser guide star (LGS) assisted adaptive optics (AO) technology. High-power narrow-linewidth lasers tuned to the sodium D2a line at 589.1591 nm are required for the LGS system to excite a layer of sodium atoms and fluoresce as a reference source in the mesosphere at 80–100 km altitude for the AO system.

However, there is currently no solid-state laser gain medium that can directly lase at 589 nm. Dye lasers are first adopted to generate 589 nm lasers, but they typically require high maintenance. With recent advances in nonlinear frequency-conversion techniques, cavity-enhanced frequency sum mixing from two single-frequency Nd:YAG lasers at 1064 nm and 1319 nm have generated a continuous wave (CW) laser of more than 50 W 589 nm, which have been developed and deployed for the astronomical community [1,2]. But such multiple-cavity systems are still complex to use. Fiber-based technologies for 589 nm laser generation have advanced in recent years. With Yb-doped photonic bandgap fibers, an up to 24.6 W single-frequency 1178 nm amplifier was reported [3] and a maximum 14.5 W 589 nm laser has been generated by single-pass frequency doubling through a PPMg:SLT crystal [4]. With polarization maintaining (PM) Raman fiber amplifier (RFA), a 44 W 1178 nm laser has been reported and a 25 W 589 nm laser was generated by frequency doubling in an external resonant cavity [5]. With coherent beam combination of three RFAs, a maximum 50.9 W 589 nm laser has been demonstrated [6]. However, the beam-combination configuration complicates the laser system. With acoustically tailored Raman gain fiber, Vergien et al. reported an 18 W single-frequency RFA at 1178 nm and there are still challenges to scale the power [7].

Most of the above-mentioned 589 nm lasers are CW. But pulsed guide star lasers can be used to gate out atmospheric Rayleigh scattering noise and avoid the fratricide effect in multiple LGS systems (see [8–10] and references therein). A solid-state guide star laser with hundred-microsecond pulses has been demonstrated and considered for future large telescopes [9, 11]. However, a fiber-based guide star laser with microsecond pulses has not been reported yet, to the best of our knowledge. Fiber-based sodium guide star lasers that have flexible pulse format will be very beneficial for the optimization of the LGS system. To increase the return flux from a LGS, repumping the sodium atoms at D2b line has been proposed [12–14]. In practice, this can be done by including a $\sim$10% fraction of the launched power at $\sim$1.71 GHz toward the blue with respect to the D2a line of sodium.

Raman fiber amplifier has shown promising for CW 589 nm guide star laser generation. A 25 W level output from a single amplifier channel was demonstrated [5]. In this paper, we report a Raman fiber amplifier-based 589 nm laser that works in both CW and pulsed formats. In the CW case, the laser produces up to 53 W output. In the pulsed case, the same laser produces square-shaped pulses with

[1] Shanghai Key Laboratory of Solid State Laser and Application, and Shanghai Institute of Optics and fine Mechanics, Chinese Academy of Sciences, Shanghai 201800, China
[2] Graduate University of the Chinese Academy of Sciences, Beijing 100049, China
*Corresponding author: e-mail: feng@siom.ac.cn

tunable repetition rate (500 Hz to 10 kHz) and duration (1 ms to 30 μs), while the peak power remains constant and as high as 84 W. The 589 nm laser is generated by resonant frequency doubling of a high-power 1178 nm single-frequency PM Raman fiber amplifier. The D2b sideband is produced directly within the doubling cavity.

2. The laser setup

The experimental setup is illustrated in Fig. 1. The seed laser is a DFB diode laser at 1178 nm with a measured linewidth of 1 MHz. The power after the fiber-coupled port is about 10 mW. Before it is amplified by two RFA stages, a high-speed phase modulator driven by a 1.71 GHz sine wave is inserted to generate two symmetrical sidebands around the fundamental frequency. A similar method has been used in [15, 16]. The insertion loss of the phase modulator is measured to be 3.3 dB. The power ratio of the side frequency to the total laser power can be continuously adjusted by changing the modulation intensity. For laser guide star application, the required power ratio is around 10% to 20%. When the modulation intensity is too high, the high harmonics sidebands would become significant. The frequency separation between the main line and sidebands is tunable by changing the modulation frequency.

Then the 1178 nm seed laser with three dominant frequency components is amplified by two RFAs that share the same configuration, as is shown in Fig. 1. The RFAs are backward pumped by 1120 nm Yb-doped fiber lasers via wavelength division multiplexers (WDM) and the residual 1120 nm laser is extracted out of the RFAs by another two WDMs. The 1120 nm linearly polarized pump sources are built in-house. For the 1st amplifier, a 20 W CW 1120 nm laser is used as the pump laser. The 1st amplifier delivers up to a 1 W 1178 nm CW laser, limited by the damage threshold of the isolator between the two amplifiers. The gain fiber is a 200 m long PM 980 fiber with an 8 steps strain distribution for SBS suppression. For the 2nd amplifier, the pump laser is a high-power linearly polarized 1120 nm laser that can work in both CW and pulsed formats. The 2nd amplifier uses 35 m PM Raman fiber with a 30 steps strain distribution to suppress the SBS effect. A small portion of the 1st amplifier output is delivered to a wavelength meter (HighFinesse WS-6) for wavelength measurement. The wavelength of amplifier output is locked to two times the sodium D2a wavelength with a PID feedback loop to control the wavelength of the DFB seed. In this way, the laser after frequency doubling is guaranteed to resonate with the D2a line.

In single-frequency RFAs, the main technical challenge for power scaling is the stimulated Brillouin scattering (SBS) effect, which generates a downshifted backward-propagating light and limits the output from the RFAs. We use a technique of applying longitudinally varied strain along the gain fiber to suppress SBS, which has been studied since the 1990s [17, 18]. The strain introduces a proportional shift of the SBS gain spectrum. Therefore, with a strain distribution, SBS light from different portions of the gain fiber is spectrally isolated and could not get amplified efficiently in other portions of the fiber. The application of the technique to narrow linewidth RFAs has been investigated intensively since 2003 [16, 19–24], and described in the literature [5, 21, 23–25].

The collimated and optically isolated 1178 nm RFA output is then coupled into a home-made bowtie-configured doubling cavity with a pair of steering mirrors and a pair of mode-matching lenses. A $3 \times 3 \times 30$ mm^3 noncritically phase matched LBO crystal with a phase-matching temperature of 40 °C is placed between two curved mirrors with a curvature radius of 50 mm. The cavity length is designed and precisely adjusted to be 157 mm, ensuring a free spectral range of 1.71 GHz. The cavity is locked to the laser using the well-established Pound–Drever–Hall (PDH) method. In this case, the main frequency and sidebands of the 1178 nm laser could resonate in the cavity simultaneously. The second harmonics of the main frequency and the sum frequency mixing of the main frequency and the sidebands are the dominant frequency-converted output. So, the generated 589 nm laser has a main frequency and two sidebands 1.71 GHz away. The blueshifted sideband will be used for repumping the sodium atoms.

3. The laser performance and discussion

The high-power 1120 nm pump laser for the 2nd 1178 nm amplifier is an integrated ytterbium-Raman fiber amplifier, the details of which have been described elsewhere [26]. Here, the 1120 nm laser is used in both CW and pulsed modes. The pulsed operation is realized by modulating the 976 nm pump diodes of both the 1120 nm seed laser and amplifier. In the pulsed case, the laser emits square-shaped pulses with pulse duration longer than 30 μs and a peak power above 375 W. Shorter pulse duration is limited by the modulation bandwidth of the driver source and the excited-state population dynamics of the Yb ions. The repetition rate is also adjustable up to 10 kHz. In the CW case, the maximum output power is 300 W. The difference is due to the laser damage threshold of the optical isolator between the 1120 nm seed and amplifier. The peak power of the 1120 nm laser in the pulsed case as well as the power in the CW case as a function of the 976 nm pump power are shown in Fig. 2.

The 1178 nm RFA is investigated first in the pulsed case. Because the response time of SRS is fast in the 100 fs scale in silica fiber, the output pulse waveform of the RFA will follow that of the pump laser, in the pulse-duration regime of interest here. In the experiment, with a 35 m variably strained fiber, the 0.8 W 1178 nm laser from the 1st amplifier is further amplified to a maximum 120 W peak power at a pump power of 375 W, as shown in Fig. 3a. SBS is well suppressed and does not reach its threshold even at maximum pump power. The backward-propagating light increases slowly, which is mainly the residual 1120 nm pump laser and amplified spontaneous Raman emission, as shown in Fig. 3b. The fraction of 1178 nm light in the

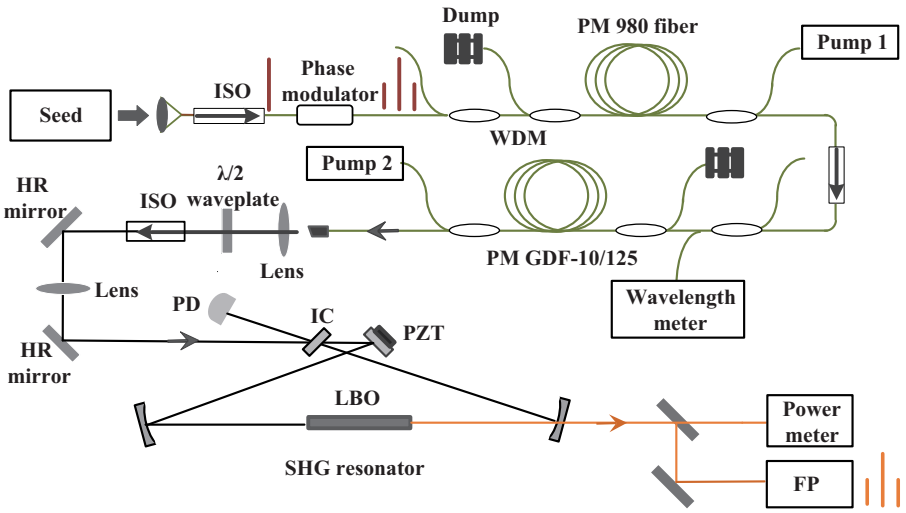

Figure 1 Schematic diagram of the laser system, including the seed laser, RFAs, and doubling cavity.

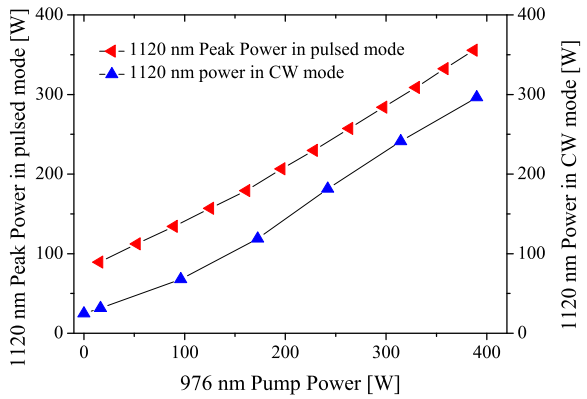

Figure 2 The peak power of the 1120 nm laser in pulsed mode and the power in CW mode as a function of the 976 nm pump power.

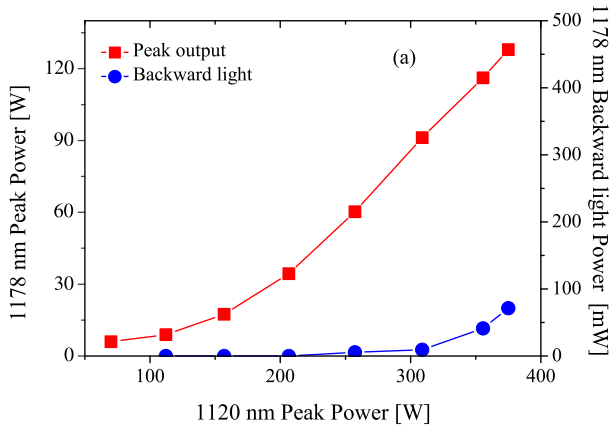

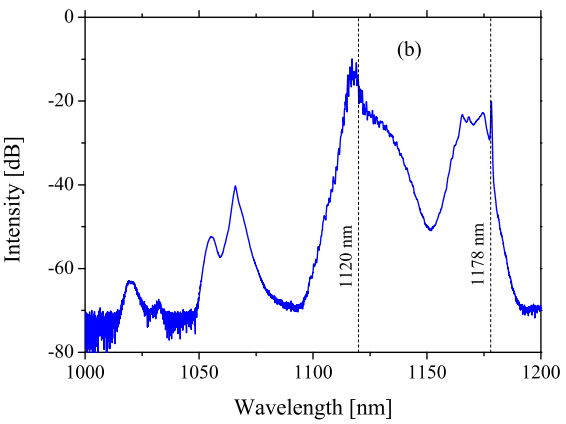

Figure 3 (a) 1178 nm peak power and backward light power as a function of the 1120 nm pump peak power. (b) Typical backward-propagating light spectrum.

backward-propagating light is calculated by spectral integration and is found to be small. The corresponding optical–optical efficiency is calculated to be 32%. The pulse width and repetition rate are adjusted in the experiments from 1 ms to 30 μs and 500 Hz to 10 kHz, respectively. These regimes of pulse duration and repetition rate are of interest for the astronomical LGS AO system to eliminate the problem of the Rayleigh scattering noise from low atmosphere [8].

Figure 4 shows typical pulse trains of the 1178 nm amplifier at different powers, where the pulse duration is about 50 μs and repetition rate is 5 kHz. With the increase of pump power, the rising and trailing edge of the pulse become smaller, which is a result of the excited-state population dynamics in the Yb gain fiber of the 1120 nm pump laser. As seen in the figure, the pulses have a smooth rising edge without relaxation oscillation spikes, which is preferable for LGS application.

The polarization extinction ratio of the output is measured to be 24 dB as a result of the all PM fiber configuration and the polarization-dependent gain of Raman scattering. The spectral purity of the laser output under different output power is checked with an optical spectral analyzer (AQ6370). Although a spectral pedestal is observed, the signal-to-noise ratio is over 50 dB at maximum power, as shown in Fig. 5.

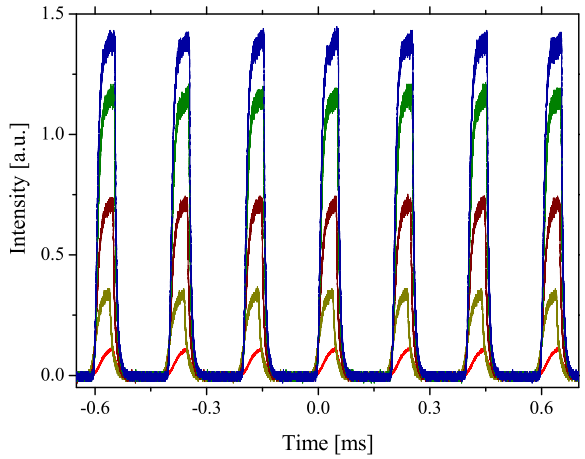

Figure 4 The pulse trains of the 1178 nm laser at different power (from the bottom to the top the output power increases). The pulse duration is about 50 μs and the repetition rate is 5 kHz.

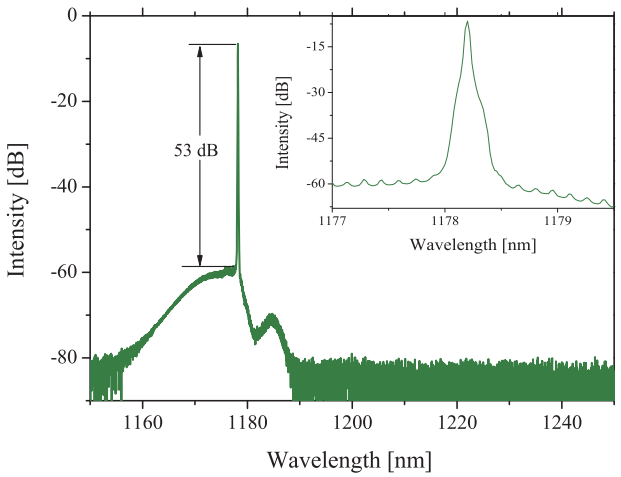

Figure 5 Spectrum of the 1178 nm RFA output at full output power, inset, spectrum with a narrow wavelength range from 1177 nm to 1079.5 nm.

The amplified single-frequency 1178 nm laser is frequency doubled in a resonant cavity described in the setup section. Figure 6 shows the pulse trains of the 589 nm output with different pulse widths under the same duty cycle of ~25%. From the bottom to the top in the figure, the pulse widths and repetitions are 30 μs with 8 kHz, 50 μs with 5 kHz, 100 μs with 2.5 kHz and 200 μs with 1.25 kHz, respectively. Correspondingly, Fig. 7a shows the 589 nm average power as a function of the fundamental 1178 nm power in different pulse durations. For instance, in the 50 μs and 5 kHz case, a laser up to 21 W 589 nm with a conversion efficiency of ~80% with respect to the incident fundamental light is obtained. Figure 7b shows the 589 nm peak power and conversion efficiency as a function of the 1178 nm peak power at a repetition rate of 5 kHz and pulse width 50 μs. The conversion efficiency reaches 81% and rolls over. We believe this is due to the thermal lens effect within the optical isolator and LBO crystal, which can be

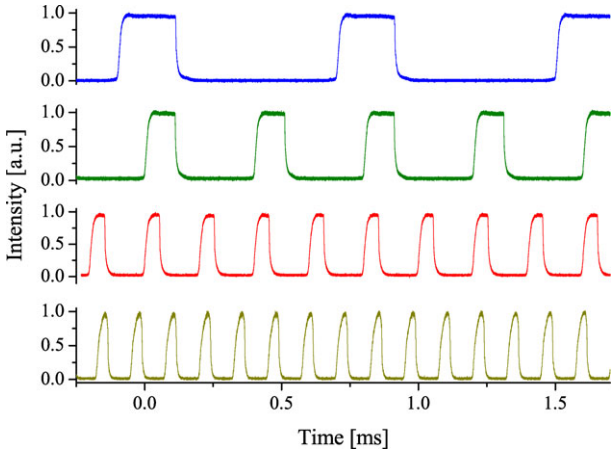

Figure 6 Pulse trains of the 589 nm laser, from the bottom to the top, the pulse widths and repetitions are 30 μs with 8 kHz, 50 μs with 5 kHz, 100 μs with 2.5 kHz and 200 μs 1.25 kHz (from the bottom to the top), respectively.

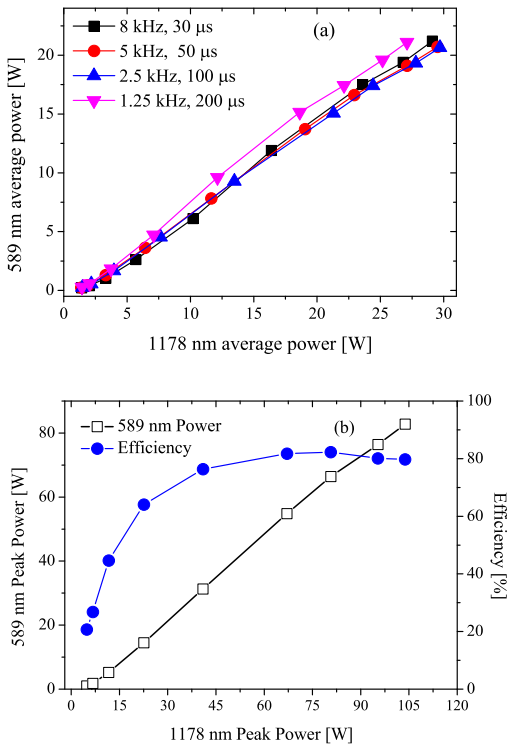

Figure 7 (a) 589 nm average output power as a function of the 1178 nm power at different repetition rates and pulse widths. (b) 589 nm peak power and conversion efficiency as a function of the 1178 nm peak power at repetition rate of 5 kHz and pulse width 50 μs.

compensated by finely adjusting the mode-matching lens. The peak power of the 589 nm reaches 84 W, which is the highest output power ever reported for a fiber-based sodium guide star laser.

The same laser setup is also investigated in the CW format. As mentioned above, in this case the maximum

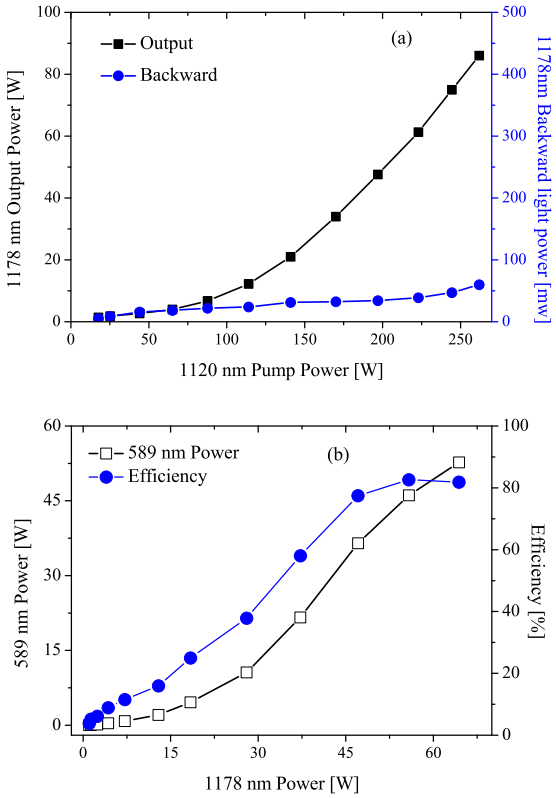

Figure 8 (a) 1178 nm power and backward light power as a function of the 1120 nm pump power in the CW case, (b) 589 nm output power and frequency doubling efficiency as a function of the fundamental 1178 nm laser power incident on the resonant doubling cavity.

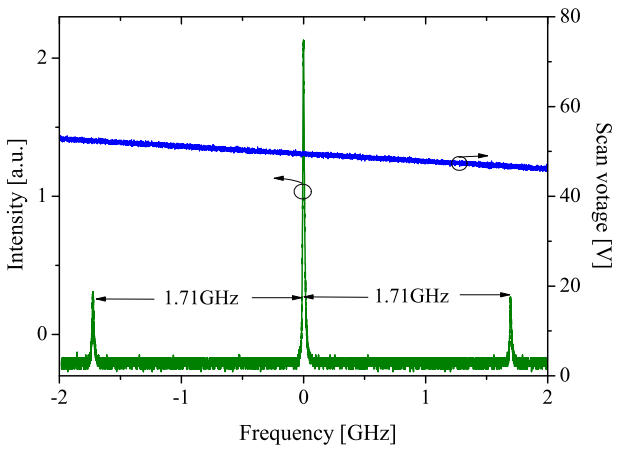

Figure 9 Spectrum of the 589 nm laser measured with a Fabry–Perot interferometer.

1120 nm pump power is only 300 W, so the 1178 nm amplifier is not in the optimized condition and produces only slightly over 80 W, as seen in Fig. 8a. An optimized amplifier should have longer gain fiber length, since the pump power is lower in the CW case. We intentionally don't

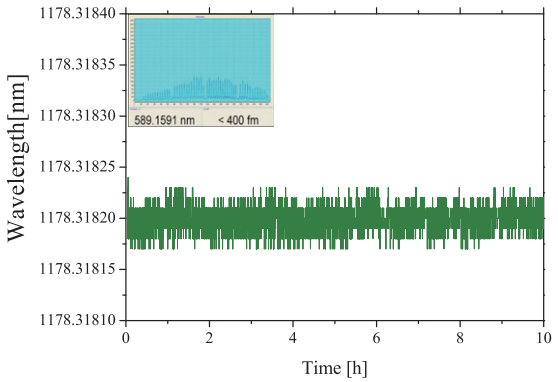

Figure 10 Wavelength-stability test with a duration of 10 h, inset, the 589 nm central wavelength and linewidth measured by the wavelength meter.

redesign the 1178 nm RFA, in order to check whether a single-laser setup could produce enough 589 nm laser in both pulsed and CW format that have been investigated in the astronomical community.

Compared with the pulsed case, in the CW case the laser has higher average power, thus has severe thermal issues. In the frequency-doubling stage, the higher power results in larger thermal lensing in the optical isolator and LBO crystal. Therefore, re-arrangement of the mode-matching lens is required to compensate the thermal lens and keep the frequency-doubling efficiency. Figure 8b shows the CW 589 nm output power and frequency-doubling efficiency as a function of the fundamental 1178 nm laser power incident on the resonant doubling cavity. A 53 W 589 nm laser is obtained with 65 W incident 1178 nm laser, which corresponds to a conversion efficiency of 82%. Better conversion efficiency is expected after further optimizing the transverse mode matching and mirror coatings. The difference between the 1178 nm amplifier output and the power incident on the cavity is due to the optical loss in the isolator, lens, and mirrors.

The spectra of the 589 nm laser are measured with a Fabry–Perot interferometer (FPI) of 4 GHz free spectral range. As mentioned above, the 1178 nm seed laser is phase modulated to generate the sidebands at 1.71 GHz. They are amplified simultaneously, and mixed in the doubling cavity. As shown in Fig. 9, there are two symmetrical frequency components that are 1.71 GHz away from the 589 nm main laser line. The blueshifted sideband is going to repump the sodium atoms at the D2b line for the laser guide star system and its amplitude can be continuously adjusted with respect to the main line. For the laser guide star application, the required power ratio is around 10% to 20%. Also, the frequency shift of sidebands can be tuned as well by changing the modulation frequency. From the same figure, one can also read the linewidth of the 589 nm laser, which is 13 MHz limited by the resolution of the FPI. The real linewidth should be well below 10 MHz, since the DFB diode laser has a linewidth of ~1 MHz and no spectral broadening could be observed after amplification.

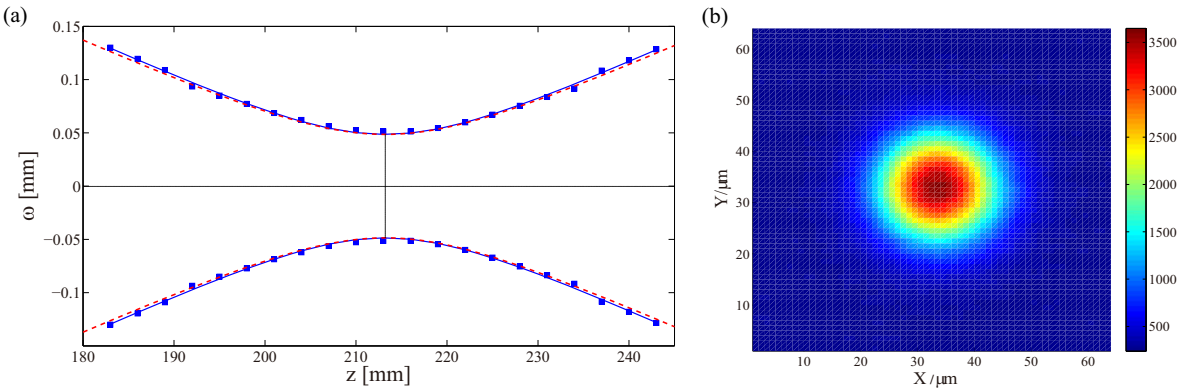

Figure 11 (a) M^2 measurement data (dots) at the full output power, which shows that the M^2 factor of the 589 nm laser is less than 1.1. The solid line is a fitting to the measured data and the dotted line represents a perfect Gaussian beam. (b) A 2D spatial beam profile of the 589 nm laser.

The 589 nm laser is locked to the D2a line of sodium by locking the fundamental laser to two times the wavelength of the D2a transition (1178.3182 nm). A wavelength meter is used to measure the wavelength, and a PID feedback loop controls the wavelength of the DFB seed laser. Figure 10 shows an example of the locking performance where the fundamental laser was locked to the wavelength of 1178.3182 nm for 10 h. The corresponding wavelength of the second-harmonic laser is locked to 589.1591 nm as shown in the inset. The linewidth reading is <400 fm (~350MHz), limited by the resolution of the wavelength meter.

Since the 1178 nm RFA is built with a single-mode fiber, and the resonant doubling cavity has itself a transverse mode cleaning function, the beam quality of the 589 nm laser is expected to be nearly diffraction limited. The M^2 factor of the 589 nm laser is measured with a commercial beam profiler (LQM-HP, PRIMES) and found to be less than 1.1. The measured data and 2D view of the beam waist profile are show in Figs. 11a and b, respectively.

4. Conclusion

We report a versatile Raman fiber amplifier-based 589 nm laser for sodium laser guide star application, which works in both pulsed and CW formats, and, therefore, offers much flexibility for astronomical application. In the pulsed case, the 1178 nm FRA produces square-shaped pulses with tunable repetition rate (500 Hz to 10 kHz) and duration (1 ms to 30 μs), while the peak power remain constant with a record peak power of 120 W. The 589 nm laser generated by frequency doubling in a resonant cavity has a peak power as high as 84 W, which leads to an average power of 21 W when the pulse duty cycle is 25%. In the CW case, the same laser setup produces up to 53 W 589 nm output, which doubles the power ever reported from a single-channel fiber-based 589 nm laser. The 1.71 GHz repumping frequency component is generated by modulating the seed laser at 1.71 GHz and designing the doubling cavity with a free spectral range of 1.71 GHz. Power scaling to the 100 W level can be done by developing a higher-power 1120 nm pump fiber laser, optimizing the 1178 nm narrow band RFA, and careful thermal management. To further scale the output power with the technology, the primary challenge is still the mitigation of SBS. In addition, the power-handling capability of the WDMs used in the Raman fiber amplifier is a technical limiting factor.

Acknowledgement. This work was supported by the National Natural Science Foundation of China (No. 61378026) and the Hundred Talent Program of the Chinese Academy of Sciences. Y.F. appreciates former colleagues at ESO for the successful research works that had been performed together.

Received: 10 March 2014, **Revised:** 23 June 2014,
Accepted: 24 June 2014

Published online: 31 July 2014

Key words: Raman fiber laser, single-frequency fiber amplifier, frequency doubling, sodium guide star.

References

[1] C. A. Denman, P. D. Hillman, G. T. Moore, J. M. Telle, J. E. Preston, J. D. Drummond, and R. Q. Fugate, Proc. SPIE **5707**, Solid State Lasers XIV: Technology and Devices, 46–49 (2005).

[2] I. Lee, M. Jalali, N. Vanasse, Z. Prezkuta, K. Groff, J. Roush, N. Rogers, E. Andrews, G. Moule, B. Tiemann, A. K. Hankla, S. M. Adkins, and C. d'Orgeville, Proc. SPIE **7015**, Adaptive Optics Systems, 70150N (2008).

[3] A. Shirakawa, C. B. Olausson, H. Maruyama, K.-i. Ueda, J. K. Lyngsø, and J. Broeng, Opt. Fiber Technol. **16**, 449–457 (2010).

[4] C. B. Olausson, A. Shirakawa, H. Maruyama, K.-i. Ueda, J. K. Lyngsø, and J. Broeng, Proc. SPIE **7580**, Fiber Lasers VII: Technology, Systems, and Applications, 758013–758013 (2010).

[5] L. Zhang, J. Hu, J. Wang, and Y. Feng, Opt. Lett. **37**, 4796–4798 (2012).

[6] L. R. Taylor, Y. Feng, and D. B. Calia, Opt. Exp. **18**, 8540–8555 (2010).
[7] C. Vergien, I. Dajani, and C. Robin, Opt. Lett. **37**, 1766–1768 (2012).
[8] R. Rampy, D. Gavel, S. Rochester, and R. Holzlöhner, Proc. SPIE **8447**, Adaptive Optics Systems III, 84474L (2012).
[9] S. M. Rochester, A. Otarola, C. Boyer, D. Budker, B. Ellerbroek, R. Holzlöhner, and L. Wang, J. Opt. Soc. Am. B **29**, 2176–2188 (2012).
[10] R. Holzlöhner, S. M. Rochester, D. Bonaccini Calia, D. Budker, T. Pfrommer, and J. M. Higbie, Proc. SPIE **8447**, Adaptive Optics Systems III, 84470H (2012).
[11] K. Wei, Y. Bo, X. Xue, X. Cheng, C. Li, J. Zuo, S. Xie, C. Rao, and Y. Zhang, Proc. SPIE **8447**, Adaptive Optics Systems III, 84471R (2012).
[12] W. Happer, Rev. Mod. Phys. **44**, 169–249 (1972).
[13] T. H. Jeys, E. Kibblewhite, R. M. Heinrichs, K. F. Wall, J. Korn, and T. C. Hotaling, Opt. Lett. **17**, 1143–1145 (1992).
[14] R. Holzlöhner, S. M. Rochester, D. Bonaccini Calia, D. Budker, J. M. Higbie, and W. Hackenberg, A&A **510**, A20 (2010).
[15] A. Friedenauer, V. Karpov, D. Wei, M. Hager, B. Ernstberger, W. R. L. Clements, and W. G. Kaenders, Proc. SPIE **8447**, Adaptive Optics Systems III, 84470F (2012).
[16] I. Dajani, C. Vergien, B. Ward, C. Robin, S. Naderi, A. Flores, and J.-C. Diels, Proc. SPIE **8604**, Nonlinear Frequency Generation and Conversion: Materials, Devices, and Applications XII, 86040N (2013).
[17] N. Yoshizawa and T. Imai, J. Lightwave Technol. **11**, 1518–1522 (1993).
[18] J. M. C. Boggio, J. D. Marconi, and H. L. Fragnito, J. Lightwave Technol. **23**, 3808–3814 (2005).
[19] R. Engelbrecht, M. Bayer, and L. P. Schmidt, "Numerical calculation of stimulated Brillouin scattering and its suppression in Raman fiber amplifiers," Conference on-CLEO/Europe, in Lasers and Electro-Optics Europe, **641** (2003).
[20] R. Engelbrecht, M. Mueller, and B. Schmauss, "SBS shaping and suppression by arbitrary strain distributions realized by a fiber coiling machine," in IEEE/LEOS Winter Topicals Meeting Series, 248–249 (2009).
[21] C. Vergien, I. Dajani, and C. Zeringue, Opt. Exp. **18**, 26214–26228 (2010).
[22] I. Dajani, C. Vergien, C. Robin, and B. Ward, Opt. Exp. **21**, 12038–12052 (2013).
[23] L. Jinyong, W. Wuming, C. Shengping, H. Jing, and X. Xiaojun, Chinese J. Lasers **31**, 606007–606001 (2011).
[24] L. Jinyong, W. Wuming, C. Shengping, X. Xiaojun, and Z. Yijun, Acta Optica Sinica **37**, 2334–2339 (2010).
[25] R. Engelbrecht, J. Lightwave Technol. **32**, 1689–1700 (2014).
[26] L. Zhang, H. Jiang, S. Cui, and Y. Feng, Opt. Lett. **39**, 1933–1936 (2014).